



1 **531-year non-growth season precipitation reconstruction in the** 2 **southeastern Tibetan Plateau**

3 Maierdang Keyimu¹, Zongshan Li^{1*}, Bojie Fu¹, Guohua Liu¹, Weiliang Chen¹, Zexin Fan³, Keyan Fang⁴,
4 Xiuchen Wu², Xiaochun Wang⁵

5 ¹State Key Laboratory of Urban and Regional Ecology, Research Center for Eco-Environmental Sciences, Chinese Academy
6 of Sciences, Beijing 100085, China

7 ²State Key Laboratory of Earth Surface Processes and Resource Ecology, Beijing Normal University, Beijing 100875, China

8 ³Xishuangbanna Tropical Botanical Garden, Chinese Academy of Sciences, Mengla 666303, China

9 ⁴Key Laboratory of Humid Subtropical Eco-Geographical Process (Ministry of Education), College of Geographical Sciences,
10 Fujian Normal University, Fuzhou 350007, China

11 ⁵College of Forestry, Northeast Forestry University, Harbin 150040, China

12 *Correspondence to:* Zongshan Li (zqli_st@rcees.ac.cn)

13 **Abstract.** Trees record climatic conditions during their growth, and tree-rings serve as a proxy to reveal the features of the
14 historical climate of a region. In this study, we collected tree-ring cores of forest hemlock (*Tsuga forrestii*) from the
15 northwestern Yunnan area of the southeastern Tibetan Plateau (SETP), and created a residual tree-ring width (TRW)
16 chronology. An analysis of the relationship between tree growth and climate revealed that precipitation during the non-growth
17 season (NGS) (from November of the previous year to February of the current year) was the most important constraining factor
18 on the radial tree growth of forest hemlock in this region. In addition, the influence of NGS precipitation on radial tree growth
19 was relatively uniform over time (1956–2005). Accordingly, we reconstructed the NGS precipitation over the period spanning
20 from A.D. 1475–2005. The reconstruction accounted for 28.5% of the actual variance during the common period 1956–2005,
21 and the leave-one-out verification parameters indicated the reliability of the reconstruction. Based on the reconstruction, NGS
22 was extremely dry during the years A.D. 1475, 1656, 1670, 1694, 1703, 1736, 1897, 1907, 1943, 1969, 1982, and 1999. In
23 contrast, the NGS was extremely wet during the years A.D. 1491, 1536, 1558, 1627, 1638, 1654, 1832, 1834–1835, and 1992.
24 Similar variations of the NGS precipitation reconstruction series and Palmer Drought Severity Index (PDSI) reconstructions
25 from surrounding regions indicated the reliability of the reconstruction. A comparison of the reconstruction with Climate
26 Research Unit (CRU) gridded data revealed that our reconstruction was representative of the NGS precipitation variability of
27 a large region in the SETP.

28 **Keywords:** Tree-rings; Winter precipitation; Reconstruction; Southeastern Tibetan Plateau



29 **1 Introduction**

30 Unravelling the past climate often relies on proxy records. As a widely used proxy material, tree-rings provide an opportunity
31 to obtain long-term climate data (Fritts, 1976; Esper et al., 2002; D'Arrigo et al., 2005; Li et al., 2011; Büntgen et al., 2011,
32 2016; Cai et al., 2014; Yang et al., 2014; Schneider et al., 2015; Wilson et al., 2016; Keyimu et al., 2021). These long-term
33 records enable us to identify the inter-annual, decadal and multi-decal variability of historical climatic conditions. They also
34 provide a reference to better understand the nature of current climatic conditions (warming/cooling, drying/wetting) and to
35 project the future regional climate, as well as the dynamic response of earth processes (e.g., forest growth, glacier
36 retreat/advance, stream flow, drought frequency, and forest fires) to climate change.

37 Being the “third pole” of the planet Earth, the Tibetan Plateau (TP) (average 4000 m a.s.l.) is particularly sensitive to climate
38 change and is one of the fastest warming places in the world (Chen et al., 2020). The average decadal temperature increase at
39 the TP is 0.33°C, which is higher than the world's average decadal temperature increase of 0.20°C (Yan and Liu, 2014).
40 Because of its geographical extent and position within the global circulation system, the TP plays a key role in regional and
41 global atmospheric circulation patterns (Griessinger et al., 2017), not only affecting the mid-latitude westerlies, but also
42 influencing the Asian monsoon circulation through its thermo-dynamical feedbacks (Duan et al., 2006; Rangwala, 2009; Wu
43 et al., 2015).

44 There are large areas of coniferous forest distributed at high altitudes in the southeastern Tibetan Plateau (SETP). Due to
45 their age and relative lack of disturbance they are a source of proxy material (tree-rings) that can be used to reveal the past
46 climatic conditions in this region (Bräuning and Mantwill, 2004; Griessinger et al., 2017; Fan et al., 2009; Fang et al., 2010;
47 Li et al., 2011; Wang et al., 2015; Li and Li., 2017; Shi et al., 2017; Huang et al., 2019; Shi et al., 2019; Keyimu et al., 2021).
48 Many dendroclimatological reconstructions of hydroclimatic variables have also been conducted in the SETP (Fan et al., 2008;
49 Zhang et al., 2015; Li et al., 2017; He et al., 2018). However, few studies have focused on the reconstruction of precipitation
50 history (He et al., 2012). The non-growth season (NGS) of vegetation (from November of the previous year to February of the
51 current year) includes the non-monsoon and pre-monsoon seasons in the SETP, and water availability during the NGS might
52 therefore have a constraining effect on radial tree growth (Linderholm and Chen, 2005). It is important to understand the long-
53 term precipitation variations during the NGS to evaluate the current trend of precipitation variation and estimate its future
54 patterns, and to determine the future responses of the forest ecosystem under the changing precipitation trend. To our
55 knowledge, however, there have been no reports of the reconstruction of NGS precipitation in this area. This hinders our
56 understanding of NGS variability from a long-term perspective.

57 In this study, we collected tree-ring cores of forest hemlock from the Xinzhu Village of northwestern Yunnan in the SETP.
58 The main objectives of the present study were to (1) identify the relationship between the radial growth of forest hemlock and
59 climate, (2) reconstruct the regional precipitation history, and (3) validate the reliability of the reconstruction. Our results not

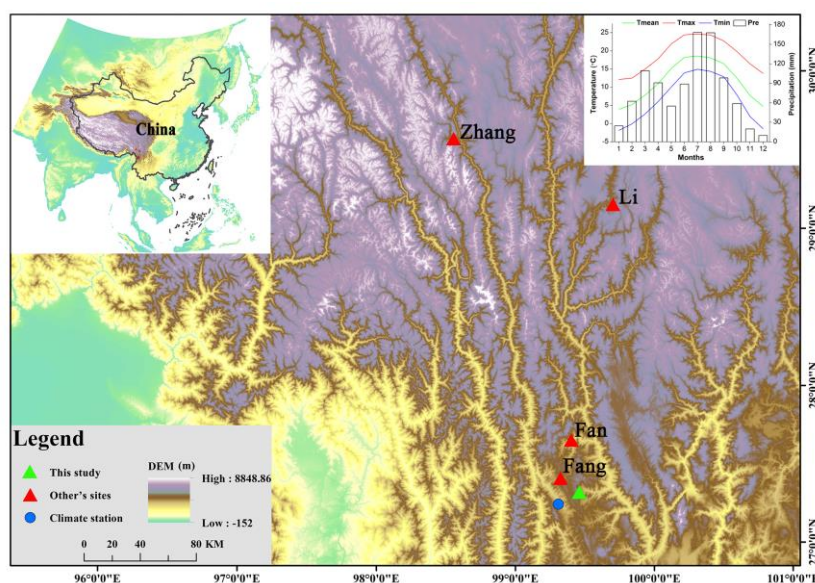


60 only improve the historical precipitation information available in the SETP, but also provide the basis to evaluate the current
61 trend of regional NGS precipitation variation, as well as the future development of regional forest growth.

62 2 Materials and methods

63 2.1 Study area and sampling sites

64 Tree-ring core samples were collected from Xinzhu Village in Lijiang County in northwestern Yunnan. The sample site was
65 in the Hengduan Mountains in the SETP (Fig. 1). The climate of the study area is regulated by a westerly circulation and the
66 monsoon circulations of the Indian and Pacific oceans. “Hengduan” means “transverse” in the Chinese language, which implies
67 that the mountains in this region lie in the transverse direction from south to north, and the area is a passageway for the Indian
68 monsoon to flow in and climb up to the TP and other parts of the mainland. The SETP is susceptible to monsoon flow and
69 atmospheric circulations (Bräuning and Mantwill, 2004). According to the Weixi meteorological station of the China
70 Meteorological Administration, which was the closest station to our sampling site, the mean annual precipitation was 953 mm
71 from 1955 to 2016. Most of the annual precipitation (Nearly 70%) concentrated in the monsoon season from May to October
72 in this region, and thus, tree growth is usually constrained by water availability during non-growth season. The coldest
73 temperature was 3.9°C in January and the warmest temperature was 18.6°C in July. Tree-ring cores of forest hemlock were
74 collected at a site that had not been impacted by anthropogenic disturbances. The elevation of the sampling site was 2,966 m
75 a.s.l. A total of 48 tree-ring cores were extracted from 48 trees using a 5.1 mm diameter increment borer. We have used one
76 sampling per tree method to improve the spatial representativity of radial tree growth. Sampling was conducted along an axis
77 perpendicular to the slope inclination to avoid the impact of tension wood (Keyimu et al., 2020).





79 **Figure 1: Map of the study area. The green triangle is the study site. The red triangles are the sites used in other studies (previous**
80 **year May – current year April PDSI reconstruction site in Fang et al., 2010; current year March – May PDSI reconstruction site in**
81 **Fan et al., 2008; current year April – June PDSI reconstruction site in Li et al., 2017; current year May - June PDSI reconstruction**
82 **site in Zhang et al., 2015). The blue dot is the meteorological station in Weixi County. The figure at upper right position is the**
83 **ombrothermic diagram of the climate variables in the study area.**

84 **2.2 Establishment of the tree-ring chronology**

85 The tree-ring samples were treated with standard dendrochronological procedures. They were first glued onto wooden holders
86 and air-dried, and then polished to a flat surface with sand paper until the tree-rings were clearly visible. The LINTAB 6.0
87 tree-ring measurement system was used to measure the tree-ring width (TRW). Crossdating was conducted visually by marking
88 each sample at each ten-year interval, and then its quality was confirmed using the COFFECHA program (Holmes, 1983).
89 Thirty-eight of the tree-ring cores were adopted for a further analysis after excluding the bad quality samples and the un-
90 crossdated samples. The tree-ring series was detrended with a negative exponential model to remove the age dependency of
91 tree growth (Cook et al., 1995). We have used the residual chronology since it removes the auto-correlation in tree-ring growth
92 and captures high frequent climate signal. The “dplR” software toolkit (Bunn, 2018) within the R software environment (R
93 Core Team 2019) was used for detrending and chronology establishment. The reliable period of the chronology was determined
94 based on the criterion of expressed population signal (EPS) > 0.85 (Wigley, 1984).

95 **2.3 Climate data**

96 Temperature and precipitation records were obtained from the Weixi meteorological station (27.17 N, 99.28 E, 2326 m a.s.l.)
97 operated by the China Meteorological Administration. Data was available for the period of 1955–2005. Climate data (including
98 the maximum, minimum and average temperatures, and precipitation) were provided by the China Meteorological Data
99 Sharing Service Platform. A self-calibrated Palmer Drought Severity Index (scPDSI) was downloaded from the 3.26e gridded
100 dataset of the Climate Research Unit (CRU) via the Royal Netherlands Meteorological Institute (KNMI) climate explorer (data
101 accessed on 23rd December, 2020) using the coordinates of the tree-ring sampling site. The range of CRU grid box is 27.0 –
102 27.5 N, 99.0 – 99.5 E.

103 **2.4 Tree growth and climate relationship analysis**

104 We analysed the relationship between climate and tree growth using Dendroclim 2002 software (Biondi and Waikul, 2004).
105 Pearson correlation values and response function values were calculated for the relationships between TRW indices and climate
106 variables for the period of 1955–2005. Due to the carry over effect of the climatic conditions of the previous-year on the current
107 year tree growth (Fritts, 1976), the tree growth – climate relationship analysis spanned a 16-month period from June of the
108 previous year to September of the current year. We also used the seasonalised climate variables because it made more eco-
109 physiological sense for growth than single months. To observe the temporal stability of the climate influence on radial tree



110 growth, we conducted a moving correlation analysis at a moving interval of 32 years. All the correlation results were considered
111 significant at the 95% confidence level.

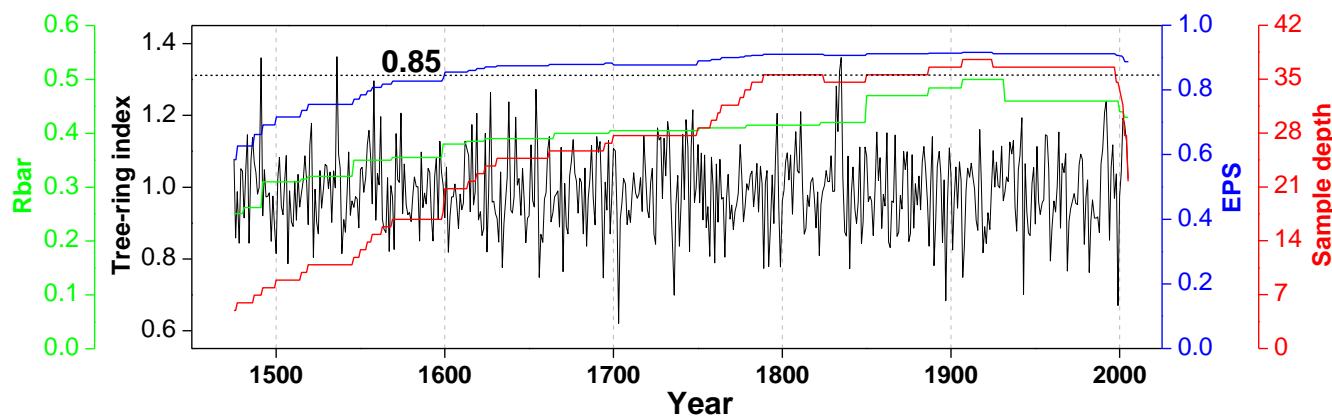
112 2.5 Climate reconstruction

113 According to the analysis of the relationship between the TRW indices and constraining climatic factors, we developed a linear
114 regression model (Cook and Kairiukstis, 1990) for the climate reconstruction. As in many other tree-ring based climate
115 reconstructions, we tested the goodness-of-fit of the model using the leave-one-out cross-validation method (Michaelsen, 1987).
116 We used the Pearson's correlation coefficient (r), explained variance (R^2), adjusted explained variance (R_{adj}^2), reduction of
117 error (RE), sign test (ST), coefficient of efficiency (CE), product mean test (Pmt) and Durbin–Watson test (DW) to evaluate
118 the fidelity of the reconstruction model (Fritts et al., 1990).

119 3. Results

120 3.1 Characteristics of the TRW chronology

121 Residual TRW chronology of forest hemlock from the investigation area was established (Fig. 2). The descriptive statistics of
122 the chronology were presented in Table 1. According to the criteria of $EPS > 0.85$, the most reliable length of the TRW
123 chronology was 405 years (A.D. 1600–2005). The EPS value of the chronology over the period of A.D. 1475–1600 was below
124 0.85. The mean correlation among tree-ring series (R_{bar}) was 0.47, and the variance in the first eigenvector (VFE) was 26 %,
125 which implied a relatively strong common signal among individual trees constituting the chronology. The relatively low inter-
126 annual variability of the chronology was expressed by the small mean sensitivity value (0.24). The EPS and SNR values
127 (average EPS and SNR were 0.86 and 5.99 for the total length chronology, respectively) further implied the existence of the
128 common signal among each individual measurement series. In general, all the statistical parameters indicated the potential
129 climate signal imprinted in our TRW chronology.



130



131 **Figure 2: Plot of tree-ring residual chronology, the running inter-correlations among cores (Rbar, the green line), expressed**
132 **population signal (EPS, the blue line) and the sample size (the red line). The Rbar and EPS were calculated using a 30-year window,**
133 **with a 15-year lag. The horizontal dashed line denotes the EPS threshold level (0.85).**

134

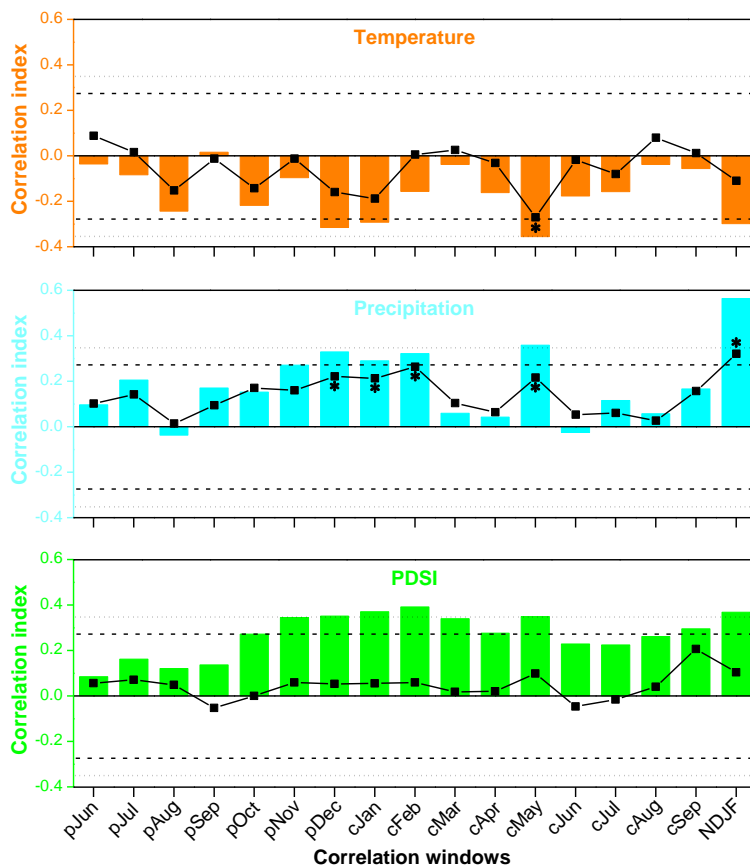
135 **Table 1. Site information, chronology statistics and results of a common interval span analysis of residual tree-ring**
136 **width (TRW) chronology from the Xinzhu Village, northwestern Yunnan in China**

Type	Location	Elevation (m)	Time length	Number of cores	SD	MS	Rbar	SNR	EPS	VFE
Tree ring	99.43°E, 27.25°N	2966	1475–2005	38	0.23	0.24	0.47	5.99	0.86	0.26

137 **Note: SD: standard deviation, MS: mean sensitivity, Rbar: mean inter-series correlation, SNR: signal-to-noise ratio, EPS: Expressed**
138 **Population Signal, VFE: Variance in first eigenvector.**

139 3.2 Tree growth and climate relationship analysis

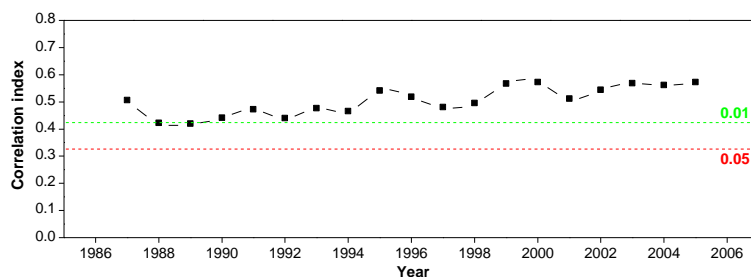
140 According to the results of the tree growth and climate relationship analyses (Fig. 3), the precipitation during the NGS was the
141 most important constraining factor ($R = 0.56$, $p < 0.001$) on the radial growth of forest hemlock in the study area. The results
142 of a response function analysis further confirmed the strong correlation between NGS precipitation and forest hemlock radial
143 growth. The results of a moving correlation analyses between TRW chronology and instrumental NGS precipitation record
144 (Fig. 4) were positively significant (at 99%) during the investigated period (1956-2005), indicating that the NGS precipitation
145 influence was stationary over time.



146

147 **Figure 3: Correlations between tree-ring indices and temperature, precipitation, and scPDSI in the correlation windows**
 148 **from previous year June to current year September, as well as in NDJF (non-growth season, NGS) for the common**
 149 **period from 1956 to 2005. The horizontal dashed and dotted lines indicate the threshold of the correlations at the 95%**
 150 **and 99% significance levels. Black line with squares denotes the results of response function analysis between tree-ring**
 151 **indices and climate variables. The asterisks next to the squares denote the significant effects ($p < 0.05$) of response**
 152 **function analyses.**

153



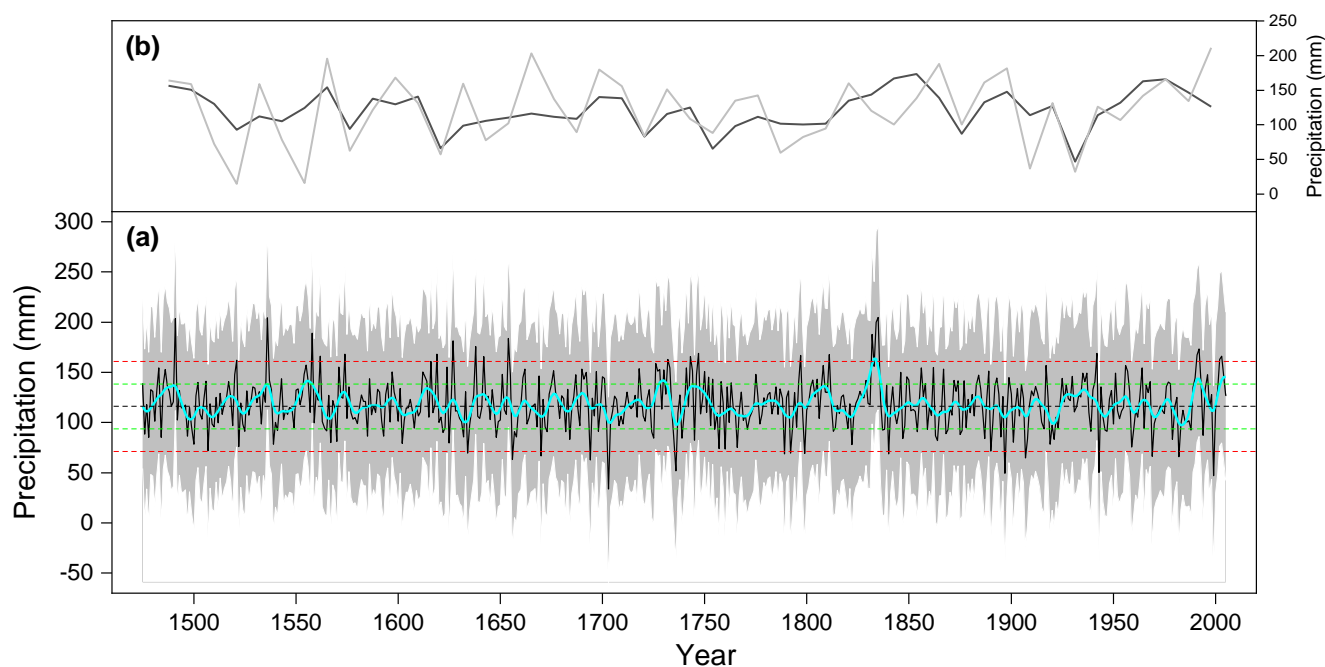
154



155 **Figure 4: The moving correlation result between tree-ring width (TRW) chronology and non-growth season (NGS) precipitation**
156 **during the period of 1956–2005. The horizontal red and green dashed lines denote the significance levels of 0.05 and 0.01, respectively.**

157 3.3 Non-growth season precipitation reconstruction

158 According to the relationship between the TRW chronology and NGS precipitation, we developed a linear regression model
159 ($y = 229.94x - 109.45$) and reconstructed the historical NGS precipitation series, which extended back to A.D. 1475 (Fig. 5a).
160 In the model, y is the NGS precipitation, and x is the TRW index. The reconstruction accounted for 28.5% of the instrumental
161 NGS precipitation variability during the common time span (1956–2005). Figure 5b shows the similarities between the
162 instrumental and reconstructed NGS precipitation series. We used a leave-one-out cross-verification method to evaluate the
163 legitimacy of the reconstruction model (Table 2). The positive RE and CE values (0.18 and 0.15, respectively) were indicative
164 of legitimacy of the reconstruction. The significant value (at 95%) of sign test implied that the model predicted values were
165 generally in line with the variation trend of instrumental values. In addition, the significant values of F test (at 99%) and PM
166 test (at 95%) further confirmed the validity of the reconstruction. Overall, the statistics indicated that the reconstruction model
167 possessed good predictive skills.



168

169 **Figure 5: Non-growth season (NGS) precipitation reconstruction from A.D. 1475 to 2005. (a). The black line is the**
170 **reconstruction series, the thick cyan line is the 11- year loess smoothed result. The horizontal black dashed line is the**
171 **mean of NGS precipitation value during from A.D. 1475–2005. The horizontal green and red dashed lines are the one**
172 **time and two times the of standard deviations of NGS precipitation, which indicated the boundaries for demonstrating**



173 the boundaries of dry and extremely dry (below mean), and wet and extreme wet (above mean) years. The grey shading
 174 indicated the 95% confidence interval of the reconstruction; (b) Instrumental (black) and reconstructed (grey) NGS
 175 precipitation during their common period of 1956–2005.

176

177 **Table 2. Leave-one-out verification statistics for the non-growth season (NGS) precipitation reconstruction**

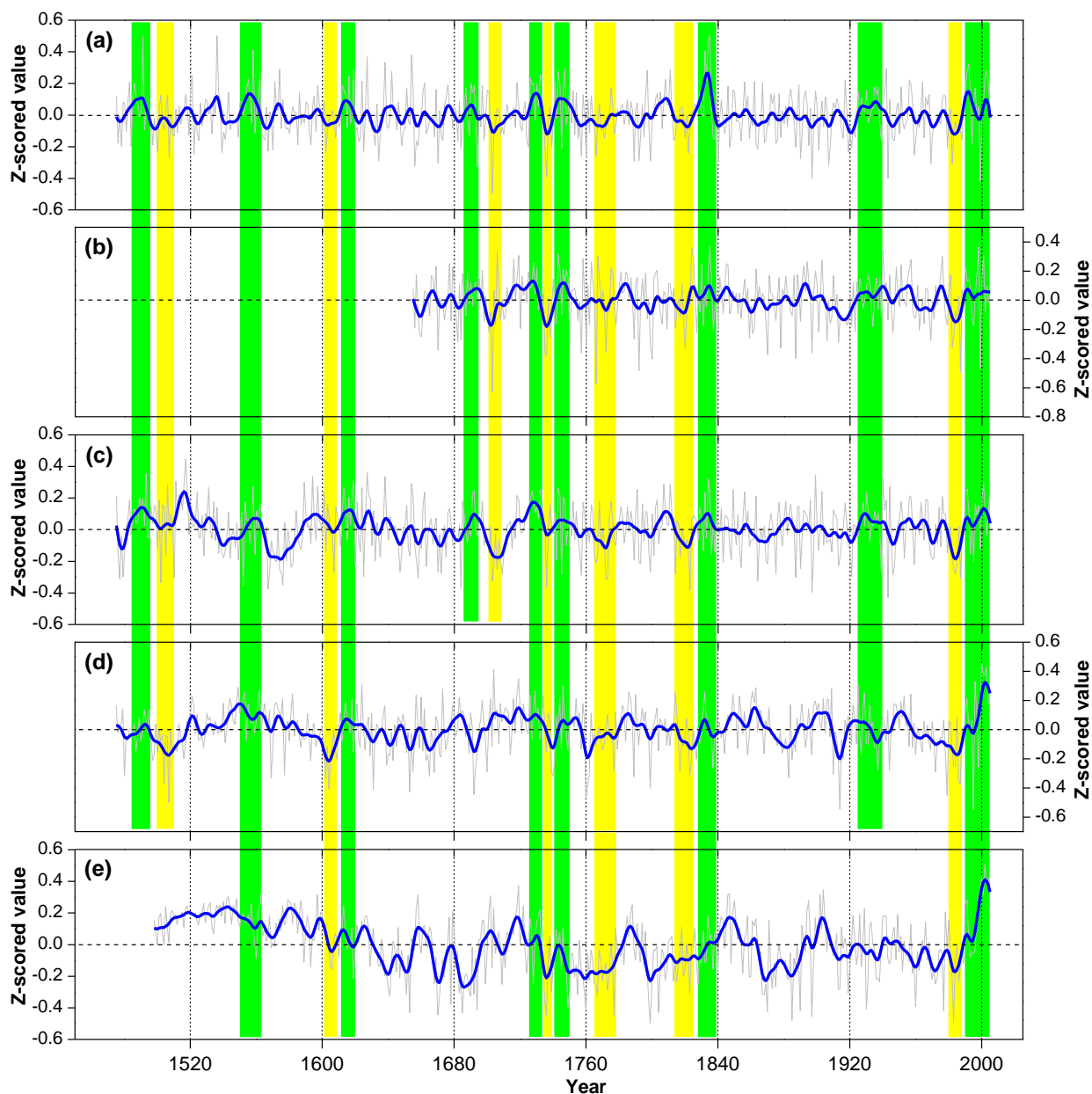
	R	R^2	R_{adj}^2	F	Sign-test	Pmt	RE	CE	DW
Calibration	0.561	0.315	0.285	–	–	–	–	–	–
Verification	0.524	0.274	0.235	18.6 ^{**}	36+/13-*	7.89*	0.18	0.15	1.68

178 **Note:** R correlation coefficient, R^2 explained variance, R_{adj}^2 is the adjusted explained variance, F F -test, Sign-test sign of paired
 179 observed and estimated departures from their mean on the basis of the number of agreements/disagreements, Pmt product mean
 180 test, RE reduction of error, CE coefficient of efficiency, DW Durbin–Watson test. * $p < 0.05$, ** $p < 0.01$

181

182 3.4 Characteristics of the NGS precipitation reconstruction

183 Figure 5a shows the reconstructed NGS precipitation over the past 531 years (A.D. 1475–2005). The mean of the reconstructed
 184 NGS precipitation series was 118.25 mm, and the standard deviation was 25.22 mm. We pre-defined the years that had NGS
 185 precipitation below 93.03 mm as dry NGS years, and below 67.81 mm as extremely dry years, whereas we defined years that
 186 had precipitation above 143.47 mm as wet NGS years, and above 168.59 mm as extremely wet NGS years. Accordingly, the
 187 NGS was extremely dry during the years A.D. 1475, 1656, 1670, 1694, 1703, 1736, 1897, 1907, 1943, 1969, 1982, and 1999.
 188 In contrast, the NGS was extremely wet during the years A.D. 1491, 1536, 1558, 1627, 1638, 1654, 1832, 1834–1835, and
 189 1992. The dry/wet NGS periods in the present reconstruction were synchronised with dry/wet periods in previously reported
 190 PDSI reconstruction from the surrounding region (Fig. 6). As shown in Fig. 7, the instrumental (a) and reconstructed (b) NGS
 191 precipitation series could represent the climatic conditions over a similar area in the SETP.

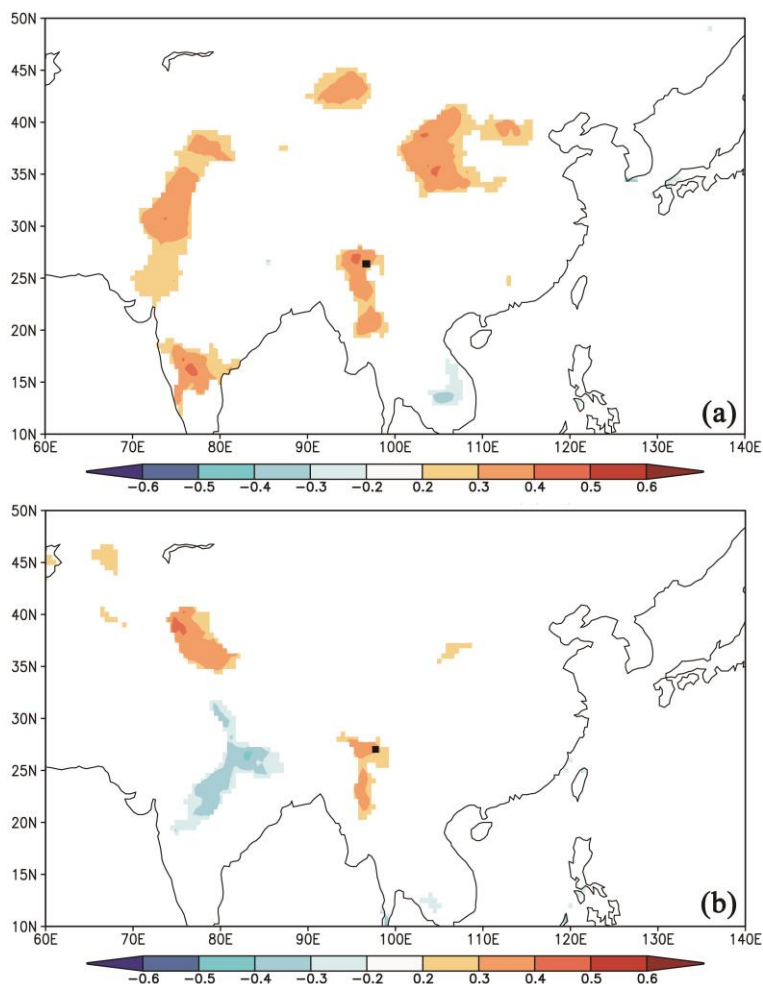


192

193 **Figure 6: Comparisons of the hydroclimatic reconstructions in different studies. (a) The non-growth season (NGS)**
194 **precipitation reconstruction in the present study. (b) The current year March – May average Palmer Drought Severity**
195 **Index (PDSI) reconstruction in Fan et al. (2008). (c) The reconstruction of average PDSI from May of the previous year**
196 **to April of the current year in Fang et al. (2010). (d) The current year May-June average PDSI reconstruction in Zhang**
197 **et al. (2015). (e) The current year April-June average PDSI reconstruction in Li et al. (2017). The green and yellow bars**
198 **show the common wet and dry periods of the different reconstructions, respectively.**



199



200

201 **Figure 7: Spatial correlations between the actual (a) and reconstructed (b) non-growth season (NGS) precipitation and**
202 **a gridded dataset of the NGS precipitation (average from November of the previous year to February of the current**
203 **year) during their overlapping periods (1956–2005). The black square indicates the location of the study site.**

204

205 4. Discussion

206 4.1 Tree growth and climate relationship

207 The results of the tree growth and climate relationship analyses suggested that the forest hemlock radial growth in the
208 northwestern Yunnan region of the SETP was strongly constrained by hydroclimatic factors. According to the Pearson



209 correlation analysis, the influence of precipitation during the NGS on radial tree growth was greater than that of any other
210 investigated climate variables and any correlation window. The response function analysis further confirmed the strong impact
211 of NGS precipitation. In addition, the results of 32-year interval of moving correlation analysis (Fig. 4) suggested the
212 temporally consistent influence of NGS precipitation on forest hemlock radial growth in this region. The importance of NGS
213 precipitation on the radial tree growth could be attributed to the fact that precipitation during the NGS compensated for the
214 soil moisture, which was crucially important for supporting tree growth in the following season (Wu et al., 2019). This is
215 because tree growth is often water stressed in the early stages of its growth in each year on the SETP when the monsoon
216 precipitation does not arrive (Bräuning and Mantwill, 2004; Zhang et al., 2015). The weak influence of precipitation on
217 regional forest hemlock growth during March and April and strong influence during May was connected with the saddle-
218 shaped monthly rainfall pattern of this area (Fig. 1). The correlations between precipitation and the TRW chronology were not
219 significant during the growth season (June-September) because an adequate water supply was available in the monsoon season.

220 Precipitation during the NGS over the SETP falls as snow. According to Sommerfeld et al. (1993) and Stadler et al. (1996),
221 the development of a snowpack insulates the underlying soil from freezing temperatures, which creates unfrozen soil
222 conditions and most of the soil processes that are active during warmer conditions also persist under snow cover, albeit at a
223 reduced rate (Edwards, 2007). Unfrozen soil can reduce the cold and frost damage to the shallow root systems of conifer trees
224 in this region (Schenk and Jackson, 2002). A reduction in the cold damage to roots decreases the energy required to form new
225 roots in the following growth year (Pederson et al., 2004), with the saved energy potentially used to initiate xylogenesis and
226 form earlywood cells. Evergreen tree species are known to carry out year-round photosynthetic activity (Oquist and Huner,
227 2003; Prats and Brodersen, 2020), albeit at a slower rate during the NGS, and therefore, the higher moisture availability
228 contributes to the carbohydrate and energy accumulation process of forest hemlock in the investigation area.

229 In contrast, the radial tree growth was negatively correlated to temperature in most correlation windows (Fig. 2). This can
230 be explained by the fact that higher temperature enhances evapotranspiration, and thus decreases water availability, which
231 eventually constrains tree growth. The negative impact of NGS temperature on radial tree growth was obvious because the
232 strengthened evaporation due to higher temperatures might reduce the moisture compensation to the soil layer and cause water
233 stress during the early stage of the following growth season.

234 **4.2 Validity of the reconstructed precipitation series**

235 We have tried to validate the fidelity of the newly reconstructed series from different aspects. Although we used the residual
236 TRW chronology in the present study, which removes autocorrelation (Cook and Kairiukstis, 1990) to capture the high
237 frequency climate signals as in Fan et al. (2008) and Chen et al. (2016), the variability of dry and wet NGS at different scales
238 was still retained in our reconstructed series. The reconstructed series in the present study demonstrated the variation in dry
239 and wet NGS years (Fig. 5). As in many other proxy based historical climate reconstruction studies, we compared our NGS



240 precipitation series with other hydroclimatic reconstructions from the surrounding areas to investigate the reliability of our
241 reconstruction. There are only countable numbers of hydroclimatic (PDSI) reconstructions in the nearby region, and not any
242 case of precipitation reconstruction. Hence, we could only compare the present NGS precipitation reconstruction with existing
243 PDSI reconstructions (Fig. 6). The compared PDSI reconstructions are of spring or early summer, because drought climate
244 during these seasons usually associated with the winter precipitation, it makes certain sense to carry out the comparative
245 analysis. The correlation coefficients between our NGS precipitation reconstruction and the PDSI reconstructions of Fan et al.
246 (2008), Fang et al. (2010), Zhang et al. (2015) and Li et al. (2017) were 0.51 ($n = 702$), 0.35 ($n = 1062$), 0.25 ($n = 1062$) and
247 0.22 ($n = 1016$) ($p < 0.001$). As can be observed from Fig. 6, there were dry and wet periods in compared reconstruction series
248 which were consistent with the NGS precipitation variabilities. These similarities indicated the reliability of our NGS
249 precipitation reconstruction to some extent. The correlation coefficients for the present reconstruction with those of Fan et al.
250 (2008) and Fang et al. (2010) were greater than those with Li et al. (2017) and Zhang et al. (2015). These differences were
251 probably due to the different distances among the study sites. Although, the major dry and wet periods were similar in the
252 hydroclimatic reconstructions referenced above, there were still certain discrepancies in duration and the strength of the dry/wet
253 climatic conditions. This is probably because of the differences in the types of hydroclimatic variables (precipitation, PDSI),
254 specific seasons reconstructed (annual, seasonal), the different tree species (species with different drought tolerances), different
255 chronology recording methods (standard chronology, residual chronology) and the geomorphic differences of the tree-ring
256 sampling sites (altitude, slope).

257 In addition, we uploaded both of the instrumental and reconstructed NGS precipitation data for the same period of 1956–
258 2005 on the KNMI website and conducted a spatial correlation analyses with the CRU gridded climate dataset. The similar
259 patterns of spatial correlation between the instrumental and reconstructed dataset (Fig. 7) indicated that the present
260 reconstruction was reliable and could represent the NGS precipitation over a large area of the SETP. Besides, the occurrence
261 of some historical great drought events in the Asian monsoon area (Cook et al., 2010), i.e., the 1756–1768 (strange parallels
262 drought), 1790, 1792–1796 (east India drought) and 1920s (post–World War I drought), matched the dry NGS periods in our
263 reconstruction, which also further confirmed the reliability of our reconstruction.

264 It should be noted that the lower sample replication prior to 1600 resulted in a reduced EPS, with a value below the commonly
265 used threshold value of 0.85 in tree-ring based climate reconstruction studies. This may affect the reliability of the
266 reconstruction before 1600. We therefore suggest caution in the interpretation of the reconstructed NGS precipitation series
267 prior to the 17th century. Nevertheless, we found similarities between the wet/dry NGS conditions before A.D. 1600 in our
268 reconstructed series and those of Fang et al. (2010) and Zhang et al. (2015) from the surrounding area (Fig. 6).



269 **5. Conclusion**

270 In this study, we investigated 531 years of residual TRW chronology of forest hemlock in the SETP, China. The climate and
271 tree growth relationship analysis showed that the TRW chronology was mostly negatively correlated with the thermal variable
272 (temperature), whereas it was positively correlated with hydroclimatic variables (precipitation and PDSI), indicating that
273 hydroclimatic conditions determined the radial growth of forest hemlock in this region. Accordingly, we derived a linear model
274 of the relationship between climate and tree growth, which accounted for 28.5% of the actual NGS precipitation variance
275 (1956–2005), and we used the model to reconstruct the historical (A.D. 1475–2005) NGS precipitation. The reconstructed
276 series showed that the NGS was extremely dry during the years A.D. 1475, 1656, 1670, 1694, 1703, 1736, 1897, 1907, 1943,
277 1969, 1982 and 1999. In contrast, the NGS was extremely wet during the years A.D. 1491, 1536, 1558, 1627, 1638, 1654,
278 1832, 1834–1835 and 1992. A comparison between the NGS precipitation reconstruction in this study and PDSI
279 reconstructions from nearby regions revealed a coherency in the timing of dry and wet episodes, suggesting the reliability of
280 our reconstruction.

281 **Data availability.** The climate reconstruction series in this study can be obtained from Zongshan Li after the paper publication.

282 **Author contributions.** ZSL and MK conceived the study; ZSL, ZXF, XCW collected the tree-ring data; MK, ZSL, ZXF, KYF,
283 XCW elaborated the methodology; MK, ZSL, WLC analysed the data; MK, ZSL led the writing of the manuscript; ZSL and
284 ZXF revised the manuscript; BJB and GHL validated the final manuscript.

285 **Competing interests.** The authors declare that they have no conflict of interest.

286 **Acknowledgement.** This work was funded by the National Key Research Development Program of China (2016YFC0502105),
287 the second Tibetan Plateau Scientific Expedition and Research (STEP) Program (2019QZKK0502). We are grateful to the
288 editor and anonymous reviewers for their valuable comments and suggestions to improve this article.

289 **References**

290 Biondi, F. and Waikul, K.: DENDROCLIM2002: a C++ program for statistical calibration of climate signals in tree ring
291 chronologies, *Comput. Geosci.*, 30(3), 303-311, <https://doi.org/10.1016/j.cageo.2003.11.004>, 2004

292 Bräuning, A. and Mantwill, B.: Summer temperature and summer monsoon history on the Tibetan Plateau during the last 400
293 years recorded by tree rings, *Geophys. Res. Lett.*, 31, L24205, <https://doi.org/10.1029/2004GL020793>, 2004

294 Bunn, A. G. and Korpela, M.: An introduction to dplR. The Comprehensive R Archive Network,
295 <https://cran.biodisk.org/web/packages/dplR/vignettes/intro-dplR.pdf>, 2018

296 Büntgen, U., Myglan, V. S., Ljungqvist, F. C., McCormick, M., Di Cosmo N., Sigl, M., Jungclauss, J., Wagner, S., Krusic, P.
297 J., Esper, J., Kaplan, J. O., de Vaan MAC., Luterbacher, J., Wacker, L., Tegel, W. and Kirilyanov, A. V.: Cooling and societal



- 298 change during the Late Antique Little Ice Age from 536 to around 660 AD, *Nat. Geosci.*, 9, 231–236,
299 <https://doi.org/10.1038/ngeo2652>, 2016
- 300 Büntgen, U., Tegel, W., Nicolussi, K., McCormick, M., Frank, D., Trouet, V., Kaplan, J. O., Herzig, F., Heussner, K. U.,
301 Wanner, H., Luterbacher, J. and Esper, J.: 2500 years of European climate variability and human susceptibility, *Science*, 331,
302 578–582, <https://doi.org/10.1126/science.1197175>, 2011
- 303 Cai, Q. F., Liu, Y., Lei, Y., Bao, G. and Sun, B.: Reconstruction of the march-august PDSI since 1703 AD based on tree rings
304 of Chinese pine (*Pinus tabulaeformis* Carr.) in the Lingkong Mountain, southeast Chinese loess Plateau, *Clim. Past.*, 10, 509–
305 521, <https://doi.org/10.5194/cp-10-509-2014>, 2014
- 306 Chen, F., Yuan, Y. J., Zhang, T. W., Shang, H.: Precipitation reconstruction for the northwestern Chinese Altay since 1760
307 indicates the drought signals of the northern part of inner Asia, *Int. J. Biometeorol.*, 60(3), 455–463.
308 <https://doi.org/10.1007/s00484-015-1043-5>, 2016
- 309 Cook, E. R. and Kairiukstis, A.: *Methods of Dendrochronology: Applications in the Environmental Sciences*, Kluwer
310 Academic Press, Dordrecht, 1990
- 311 Cook, E. R., Anchukaitis, K. J., Buckley, B. M., D'Arrigo, R. D., Jacoby, G. C. and Wright, W. E.: Asian monsoon failure and
312 megadrought during the last millennium, *Science*, 328(5977), 486–489, <https://doi.org/10.1126/science.1185188>, 2016
- 313 Cook, E. R., Briffa, K. R., Meko, D. M., Graybill, D. A. and Funkhouser, G.: The 'segment length curse' in long tree-ring
314 chronology development for palaeoclimatic studies, *Holocene*, 5(2), 229–237. <https://doi.org/10.1177/095968369500500211>,
315 1995
- 316 D'Arrigo, R. D., Mashig, E., Frank, D. C., Wilson, R. J. S. and Jacoby, G. C.: Temperature variability over the past millennium
317 inferred from Northwestern Alaska tree rings, *Clim. Dynam.*, 24, 227–236. <https://doi.org/10.1007/s00382-004-0502-1>, 2005
- 318 Duan, K., Yao, T. and Thompson, L.: Response of monsoon precipitation in the Himalayas to global warming, *J. Geophys.*
319 *Res.*, 111, D19110. <https://doi.org/10.1029/2006JD007084>, 2006
- 320 Edwards, A. C., Scalenghe, R., Freppaz, M.: Changes in the seasonal snow cover of alpine regions and its effect on soil
321 processes: a review. *Quat. Int.*, 162–163, 172–181. <https://doi.org/10.1016/j.quaint.2006.10.027>, 2007
- 322 Esper, J.: 1300 years of climatic history for Western Central Asia inferred from tree-rings, *Holocene*, 12(3), 267–277.
323 <https://doi.org/10.1191/0959683602hl543rp>, 2002
- 324 Fan, Z. X., Bräuning, A. and Cao, K. F.: Tree-ring based drought reconstruction in the central Hengduan Mountains region
325 (China) since AD 1655, *Int. J. Climatol.*, 28, 1879–1887, <https://doi.org/10.1002/joc.1689>, 2008
- 326 Fan, Z. X., Bräuning, A., Yang, B. and Cao, K. F.: Tree ring density-based summer temperature reconstruction for the central
327 Hengduan Mountains in southern China, *Global Planet. Change*, 65 (1–2), 1–11.
328 <https://doi.org/10.1016/j.gloplacha.2008.10.001>, 2009



- 329 Fang, K. Y., Gou, X. H., Chen, F., Li, J. B., D'Arrigo, R., Cook, E. D., Yang, T. and Davi, N.: Reconstructed droughts for the
330 southeastern Tibetan Plateau over the past 568 years and its linkages to the Pacific and Atlantic Ocean climate variability,
331 *Clim. Dyn.*, 35(4), 577–585. <https://doi.org/10.1007/s00382-009-0636-2>, 2010
- 332 Fritts, H. C., Guiot, J. and Gordon, G. A.: Verification. In: Cook E and Kairiukstis LA, eds., *Methods of Dendrochronology:*
333 *Applications in the Environmental Sciences*. Dordrecht, Kluwer Academic Publishers, 178-184, 1990
- 334 Fritts, H. C.: *Tree rings and climate*. Academic Press, London, 1976
- 335 Griessinger, J., Bräuning, A., Helle, G., Hochreuther, P. and Schleser, G.: Late Holocene relative humidity history on the
336 southeastern Tibetan plateau inferred from a tree ring $\delta^{18}O$ record: recent decrease and conditions during the last 1500 years,
337 *Quat. Int.*, 430, 52–59, <http://dx.doi.org/10.1016/j.quaint.2016.02.011>, 2017
- 338 He, H. M., Bräuning, A., Griessinger, J., Hochreuther, P. and Wernicke, J.: May–June drought reconstruction over the past
339 821 years on the southcentral Tibetan Plateau derived from tree-ring width series, *Dendrochronologia*, 47, 48–57,
340 <https://doi.org/10.1016/j.dendro.2017.12.006>, 2018
- 341 He, H. M., Yang, B., Bräuning, A., Wang, J. L. and Wang, Z. Y.: Tree-ring derived millennial precipitation record for the
342 south-central Tibetan plateau and its possible driving mechanism, *Holocene*, 23 (1), 36-45,
343 <https://doi.org/10.1177/0959683612450198>, 2012
- 344 Holmes, R. L.: Computer-assisted quality control in tree-ring dating and measurement, *Tree-ring Bulletin*, 43, 69-75, 1983
- 345 Huang, R., Zhu, H. F., Liang, E. Y., Liu, B., Shi, J. F., Zhang, R. B., Yuan, Y. J., Griessinger, J.: A tree ring-based winter
346 temperature reconstruction for the southeastern Tibetan Plateau since 1340 CE, *Clim. Dyn.* 53, 3221-3233.
347 <https://doi.org/10.1007/s00382-019-04695-3>, 2019
- 348 Keyimu, M., Li, Z. S., Liu, G. H., Fu, B. J., Fan, Z. X., Wang, X. C. Zhang, Y. D., Halik, U.: Tree-ring based minimum
349 temperature reconstruction on the southeastern Tibetan Plateau, *Quat. Sci. Rev.*, 251, 106712.
350 <https://doi.org/10.1016/j.quascirev.2020.106712>, 2021
- 351 Keyimu, M., Wei, J. S., Zhang, Y. X., Zhang, S., Li, Z. S., Ma, K. M., Fu, B. J.: Climate signal shift under the influence of
352 prevailing climate warming – Evidence from *Quercus liaotungensis* on Dongling Mountain, Beijing, China,
353 *Dendrochronologia*, 60, 125683. <https://doi.org/10.1016/j.dendro.2020.125683>, 2020
- 354 Li, J. B., Shi, J. F., Zhang, D. D., Yang, B., Fang, K. Y. and Yue, P. H.: Moisture increase in response to high-altitude warming
355 evidenced by tree-rings on the southeastern Tibetan Plateau, *Clim. Dyn.*, 48, 649–660. [https://doi.org/10.1007/s00382-016-](https://doi.org/10.1007/s00382-016-3101-z)
356 [3101-z](https://doi.org/10.1007/s00382-016-3101-z), 2017
- 357 Li, T., Li, J.B.: A 564-year annual minimum temperature reconstruction for the east central Tibetan Plateau from tree rings,
358 *Glob. Planet. Change* 157, 165-173. <https://doi.org/10.1016/j.gloplacha.2017.08.018>, 2017.



- 359 Li, Z. S., Zhang, Q. B. and Ma, K. P.: Tree-ring reconstruction of summer temperature for A.D. 1475–2003 in the central
360 Hengduan Mountains, northwestern Yunnan, China, *Clim. Change*, 110(1-2), 455-467, [https://doi.org/10.1007/s10584-011-](https://doi.org/10.1007/s10584-011-0111-z)
361 [0111-z](https://doi.org/10.1007/s10584-011-0111-z), 2011
- 362 Liang, E. Y., Liu, X. H., Yuan, Y. J., Qin, N. S., Fang, X. Q., Huang, L., Zhu, H. F., Wang, L. L. and Shao, X. M.: The 1920s
363 drought reconstructed by tree rings and historical documents in the semi-arid and arid areas of northern China, *Clim. Change*,
364 79, 403–432. <https://doi.org/10.1007/s10584-006-9082-x>, 2006
- 365 Linderholm, H. W., Chen, D.: Central Scandinavian winter precipitation variability during the past five centuries reconstructed
366 from *Pinus sylvestris* tree rings, *Boreas* 34, 43–52, 2005
- 367 Michaelsen, J.: Cross-validation in statistical climate forecast models, *J. Clim. App. Meteorol.*, 26, 1589-1600, 1987
- 368 R: A language and environment for statistical computing. R Foundation for Statistical Computing, Vienna, Austria. URL
369 <https://www.R-project.org/>, 2019
- 370 Oquist, G., Huner, N. P.: Photosynthesis of overwintering evergreen plants, *Annu. Rev. Plant Biol.* 54, 329–355.
371 <https://doi.org/10.1146/annurev.arplant.54.072402.115741>, 2003
- 372 Prats, K. A., Brodersen, C. R.: Seasonal coordination of leaf hydraulics and gas exchange in a wintergreen fern, *AoB Plants*,
373 12(6), 1–13. <https://doi.org/10.1093/aobpla/plaa048>, 2020
- 374 Pederson, N., Cook, E. R., Jacoby, G. C., Peteet, D. M., Griffin, K. L.: The influence of winter temperatures on the annual
375 radial growth of six northern range margin tree species, *Dendrochronologia* 22 (1), 7–29.
376 <https://doi.org/10.1016/j.dendro.2004.09.005>, 2004
- 377 Rangwala, I., Miller, J. R. and Xu, M.: Warming in the Tibetan Plateau: Possible influences of the changes in surface water
378 vapor, *Geophys. Res. Lett.*, 36, L06703, <https://doi.org/10.1029/2009GL037245>, 2009
- 379 Schenk, H. J., & Jackson, R. B.: The global biogeography of roots. *Ecol. Monogr.* 72, 311–328. [https://doi.org/10.1890/0012-](https://doi.org/10.1890/0012-9615(2002)072[0311:TGBOR]2.0.CO;2)
380 [9615\(2002\)072\[0311:TGBOR\]2.0.CO;2](https://doi.org/10.1890/0012-9615(2002)072[0311:TGBOR]2.0.CO;2), 2002
- 381 Schneider, L., Smerdon, J. E., Büntgen, U., Wilson, R. J. S., Myglan, V. S., Kirilyanov, A. V. and Esper, J.: Revising mid-
382 latitude summer temperatures back to AD 600 based on a wood density network, *Geophys. Res. Lett.*, 42, 4556-4562.
383 <https://doi.org/10.1002/2015GL063956>, 2015
- 384 Shi, C. M., Sun, C., Wu, G. C., Wu, X. C., Chen, D. L., Masson-Delmotte, V., Li, J. P., Xue, J. Q., Li, Z. S., Ji, D. Y., Zhang,
385 J., Fan, Z. X., Shen, M. G., Shu, L. F., Ciais, P.: Summer temperature over Tibetan Plateau modulated by Atlantic multi-
386 decadal variability, *J. Clim.* 32, 4055-4067. <https://doi.org/10.1175/JCLI-D-17-0858.1>, 2019
- 387 Shi, S. Y., Li, J. B., Shi, J. F., Zhao, Y. S. and Huang, G.: Three centuries of winter temperature change on the southeastern
388 Tibetan plateau and its relationship with the Atlantic Multidecadal Oscillation, *Clim. Dynam.*, 49, 1305-1319.
389 <https://doi.org/10.1007/s00382-016-3381-3>, 2017



- 390 Sommerfeld, R. A., Mosier, A. R., Musselman, R. C.: CO₂, CH₄ and N₂O flux through a Wyoming snowpack and implications
391 for global budget, *Nature*, 361, 140–142, <https://doi.org/10.1038/361140a0>, 1993
- 392 Stadler, D., Wunderli, H., Auckenthaler, A., Fluhler, H.: Measurement of frost induced snowmelt runoff in a forest soil, *Hydrol.*
393 *Process.*, 10, 1293–1304, [https://doi.org/10.1002/\(SICI\)1099-1085\(199610\)10:10<1293::AID-HYP461>3.0.CO;2-I](https://doi.org/10.1002/(SICI)1099-1085(199610)10:10<1293::AID-HYP461>3.0.CO;2-I), 1996
- 394 Wang, J. L., Yang, B., Jungqvist, F. C.: A millennial summer temperature reconstruction for the eastern Tibetan Plateau from
395 tree-ring width, *J. Clim.* 28(13), 5289–5304. <https://doi.org/10.1175/JCLI-D-14-00738.1>, 2015
- 396 Wigley, T. M., Briffa, K. R., and Jones, P. D.: On the average value of correlated time series, with applications in
397 dendroclimatology and hydrometeorology, *J. Clim. Appl. Meteorol.*, 23, 201–213, [https://doi.org/10.1175/1520-0450\(1984\)0232.0.CO;2](https://doi.org/10.1175/1520-0450(1984)0232.0.CO;2), 1984
- 399 Wilson, R., Anchukaitis, K., Briffa, K. R., Büntgen, U., Cook, E., D'Arrigo, R., Davi, N., Esper, J., Frank, D., Gunnarson, B.,
400 Hegerl, G., Helama, S., Klesse, S., Krusic, P.J., Linderholm, H.W., Myglan, V., Osborn, T.J., Rydval, M., Schneider, L.,
401 Schurer, A., Wiles, G., Zhang, P. and Zorita, E.: Last millennium northern hemisphere summer temperatures from tree rings:
402 Part I: the long term context, *Quat. Sci. Rev.*, 134, 1–18. <https://doi.org/10.1016/j.quascirev.2015.12.00>, 2016
- 403 Wu, G., Duan, A., Liu, Y., Mao, J., Ren, R., Bao, Q., He, B., Liu, B. and Hu, W.: Tibetan Plateau climate dynamics: recent
404 research progress and outlook, *Natl. Sci. Rev.*, 2, 100–116, <https://doi.org/10.1093/nsr/nwu045>, 2015
- 405 Wu, X. C., Li, X. Y., Liu, H. Y., Ciais, P., Li, Y. Q., Xu, C. Y., Babst, F., Guo, W. C., Hao, B. Y., Wang, P., Huang, Y. M.,
406 Liu, S. M., Tian, Y. H., He, B. and Zhang, C. C.: Uneven winter snow influence on tree growth across temperate China, *Glob.*
407 *Change Biol.*, 25, 144–154. <https://doi.org/10.1111/gcb.14464>, 2019
- 408 Yan, L. and Liu, X.: Has climatic warming over the Tibetan Plateau paused or continued in recent years? *J. Earth Ocean Atmos.*
409 *Sci.*, 1, 13–28, 2014
- 410 Yang, B., Qin, C., Wang, J., He, M., Melvin, T. M., Osborn, T. J.: A 3,500-year tree-ring record of annual precipitation on the
411 northeastern Tibetan Plateau, *Proc. Natl. Acad. Sci. U. S. A.*, 111(8), 2903–2908. <https://doi.org/10.1073/pnas.1319238111>,
412 2014
- 413 Zhang, Q. B., Evans, M. N., Lyu, L. X.: Moisture dipole over the Tibetan Plateau during the past five and a half centuries, *Nat.*
414 *Commun.*, 6, 8062. <https://doi.org/10.1038/ncomms9062>, 2015